Platinum Metal Thioether Macrocyclic Complexes: Synthesis, Electrochemistry, and Single-crystal *X*-Ray Structures of *cis*-$[RhCl_2L^2]PF_6$ and *trans*-$[RhCl_2L^3]PF_6$ (L^2 = 1,4,8,11-tetrathiacyclotetradecane, L^3 = 1,5,9,13-tetrathiacyclohexadecane)†

Alexander J. Blake, Gillian Reid, and Martin Schröder *
Department of Chemistry, University of Edinburgh, West Mains Road, Edinburgh EH9 3JJ

Reaction of $RhCl_3$ with 1 mol equivalent of L [1,4,7,10-tetrathiacyclododecane (L^1), 1,4,8,11-tetrathiacyclotetradecane (L^2), and 1,5,9,13-tetrathiacyclohexadecane (L^3)] in refluxing MeOH affords the rhodium(III) complex cations $[RhCl_2L]^+$. The complex *cis*-$[RhCl_2L^2]PF_6$ crystallises in the monoclinic space group *C*2/*c*, with *a* = 10.746(8), *b* = 11.298(5), *c* = 15.708(8) Å, β = 92.00(5)°, and *Z* = 4. A single-crystal *X*-ray structure shows the cation sitting on a crystallographically imposed C_2 axis with octahedral Rh^{III} bound to two mutually *cis* chloro ions [Rh–Cl 2.383 6(12) Å]. The tetrathia macrocycle adopts a folded conformation with S(1) and S(8) *trans* to chloride, Rh–S(1) 2.287 0(12) and Rh–S(4) 2.327 5(12) Å. The *trans* isomer has not been detected spectroscopically in reactions of Rh^{III} with L^1 and L^2; the tendency of these ligands to co-ordinate to second- and third-row transition-metal ions to form *cis* complexes is ascribed to the large radii of these metal ions relative to the cavity size of the 12-and 14-membered rings. This is confirmed by structural analysis of $[RhCl_2L^3]PF_6$ which shows mutually *trans* chloro ligands, Rh–Cl 2.339 1(22) Å. The complex *trans*-$[RhCl_2L^3]PF_6$ crystallises in the monoclinic space group *C*2/*c*, with *a* = 11.950 7(20), *b* = 11.105 5(15), *c* = 16.206 7(18) Å, β = 95.197(21)°, and *Z* = 4. The single-crystal *X*-ray structure shows Rh^{III} on an inversion centre with the six-membered chelate rings of the macrocycle adopting alternate chair and twist-boat conformations, Rh–S(1) 2.348 3(25) and Rh–S(5) 2.348 3(27) Å.

As part of a study of the binding of polythioether macrocycles to platinum-group metal ions,[1] we have investigated the incorporation of Rh^{III} into the 12-, 14-, and 16-membered ring tetrathia macrocycles 1,4,7,10-tetrathiacyclododecane (L^1), 1,4,8,11-tetrathiacyclotetradecane (L^2), and 1,5,9,13-tetrathiacyclohexadecane (L^3). The insertion of Rh^{III} into L^2 has been reported previously by Travis and Busch[2] to afford a dichloro complex assigned as *cis*-$[RhCl_2L^2]^+$. The solid-state structure of the metal-free ligand L^2 shows the lone pairs on S directed away from the macrocyclic hole suggesting a tendency to exodentate binding of metal ions.[3] Indeed, exodentate co-ordination of the ligand has been observed in $[Nb_2Cl_{10}L^2]$,[4] $[Hg_2Cl_4L^2]$,[5] and $[M_2Cl_2(C_5Me_5)_2L^2]^{2+}$ (M = Rh or Ir),[1] while endodentate binding occurs in the square-planar complexes of Ni^{II},[6] Cu^{II},[7] and Pd^{II}.[1] The copper(I) species $[CuL^2]^+$ shows a chain structure with the tetrahedral metal centre bound to three thia donors of one ligand and one thia donor of another macrocycle.[8]

In view of the observation that cyclam (1,4,8,11-tetraazacyclotetradecane) binds Rh^{III} to afford *cis*- and *trans*-$[RhCl_2(cyclam)]^+$ depending upon the reaction conditions,[9] we wished to determine whether it might be possible to generate the complex *trans*-$[RhCl_2L^2]^+$. In addition, the synthesis of macrocyclic complexes incorporating two mutually *cis* labile sites is of particular interest with respect to potential carbonyl[10] and hydride[11] insertion reactions at a metal template.

Related 16-membered tetrathia macrocycles have been shown recently to bind Mo^0 and Mo^{II} to give the *trans* complexes $[MoL(CO)_2]$ and $[MoX_2L]$ (X = Cl or Br; L = 3,3,7,7,11,11,15,15-octamethyl-1,5,9,13-tetrathiacyclohexadecane).[12] In view of the smaller ionic radius of Rh^{III} relative to Mo^0 and Mo^{II}, we argued that the 16-membered macrocycle 1,5,9,13-tetrathiacyclohexadecane, L^3, would be capable of binding Rh^{III} to yield a *trans* complex.

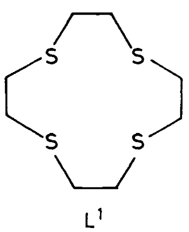

L^1

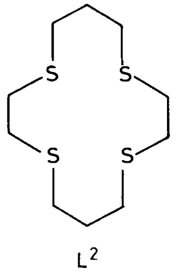

L^2

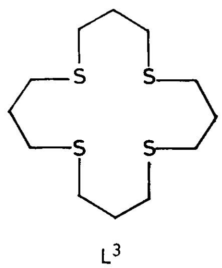

L^3

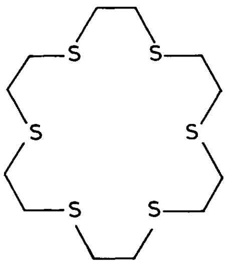

L^4

Results and Discussion

Reaction of $RhCl_3{\cdot}3H_2O$ with L^1, L^2, or L^3 in refluxing MeOH under N_2 afforded a bright yellow solution. Addition of an

---

† *cis*-Dichloro(1,4,8,11-tetrathiocyclotetradecane-$S^1S^4S^8S^{11}$)-rhodium hexafluorophosphate and *trans*-dichloro(1,5,9,13-tetrathiacyclohexadecane-$S^1S^5S^9S^{13}$)rhodium hexafluorophosphate.

Supplementary data available: see Instructions for Authors, *J. Chem. Soc., Dalton Trans.*, 1989, Issue 1, pp. xvii—xx.

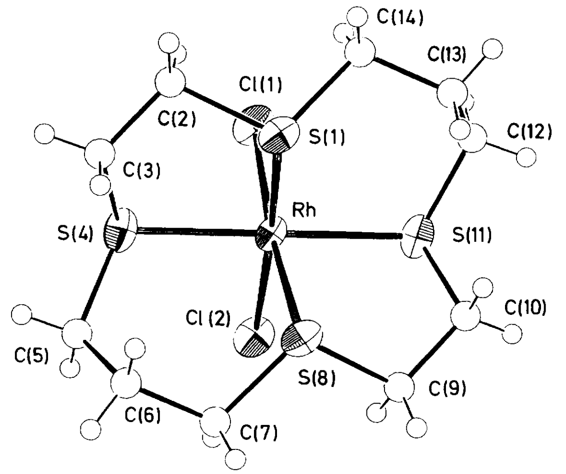

Figure 1. Single-crystal *X*-ray structure of *cis*-$[RhCl_2L^2]^+$ with the numbering scheme adopted. S(8)—C(14) are related to S(1)—C(7) by the crystallographic two-fold axis, as are Cl(1) and Cl(2)

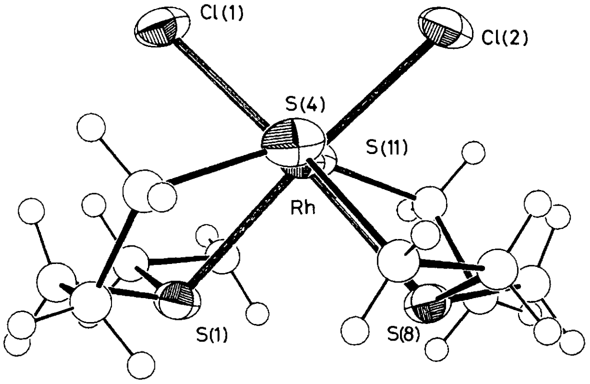

Figure 2. Single-crystal *X*-ray structure of *cis*-$[RhCl_2L^2]^+$ with the numbering scheme adopted (alternative view)

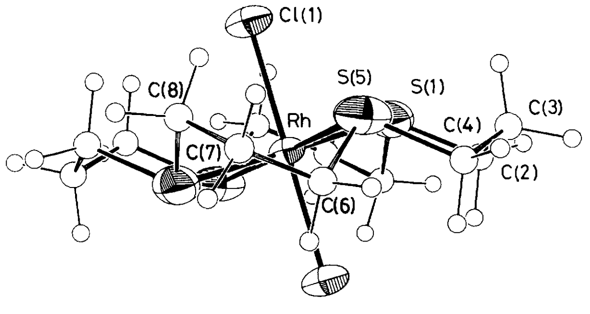

Figure 3. Single-crystal *X*-ray structure of *trans*-$[RhCl_2L^3]^+$ with the numbering scheme adopted

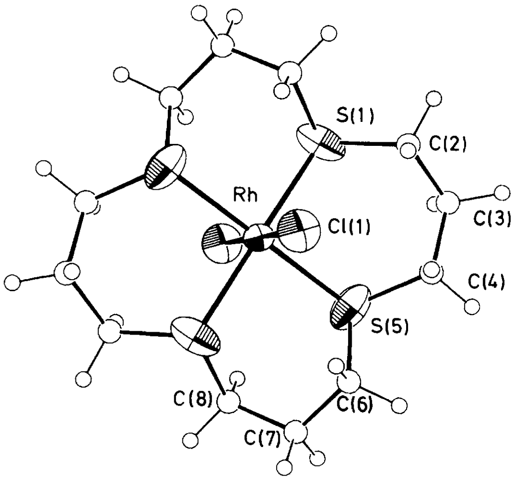

Figure 4. Single-crystal *X*-ray structure of *trans*-$[RhCl_2L^3]^+$ with the numbering scheme adopted (alternative view)

excess of NH_4PF_6 in MeOH to the filtered solution gave a yellow precipitate which was recrystallised from MeCN. Elemental analysis of the product indicated the formation of the complexes $[RhCl_2L]PF_6$. Replacement of NH_4PF_6 with $NaBPh_4$ in the above preparation led to isolation of the corresponding BPh_4^- salts.

Fast-atom-bombardment mass spectroscopy of $[RhCl_2L^2]PF_6$ showed positive-ion peaks with the correct isotopic distributions at *m/z* 441, 406, and 370 corresponding to $[^{103}Rh^{35}Cl_2L^2]^+$, $[^{103}Rh^{35}ClL^2]^+$, and $[^{103}RhL^2 - H]^+$ respectively *via* successive loss of chloride ion. The ^1H n.m.r. spectrum of the BPh_4^- salt confirmed the ratio of one BPh_4^- anion to one L^2 ligand, while the ^{13}C n.m.r. spectrum in CD_3CN showed five resonances for the methylene centres of the macrocycle at δ 38.31, 30.10, 29.95, 29.85, and 23.84 p.p.m. indicating the presence of only one isomer in solution involving *cis*-dichloro ligands. The assignment of the cation as a *cis* isomer was suggested also by u.v.–visible spectral data which showed *d–d* absorption bands at $\lambda_{max.} = 362$ ($\varepsilon_{max.} = 949$), 319 (765), and a charge-transfer band at 260 nm ($\varepsilon_{max.} = 10\,370$ dm^3 mol^{-1} cm^{-1}). The magnitudes of the absorption coefficients for the *d–d* transitions are consistent with the lower-symmetry *cis* isomer; octahedral d^6 complexes tend to show[9] lower absorption coefficients in *trans* configurations. The i.r. spectrum of the complex shows several weak bands in the range 270—350 cm^{-1}. It is difficult to assign these bands since both Rh–Cl and Rh–S stretching vibrations, ν(Rh–Cl) and ν(Rh–S), occur in this region of the spectrum.

In order to confirm the stereochemistry and conformation of the complex and to obtain bond-length distributions, a single-crystal *X*-ray structural determination was undertaken. Single crystals of $[RhCl_2L^2]PF_6$ were obtained by recrystallisation of the complex from MeCN. Figures 1 and 2 give two views of the complex cation. The structural analysis confirms the *cis* configuration of the complex [Rh–Cl 2.383 6(12), Rh–S(1) 2.287 0(12), and Rh–S(4) 2.327 5(12) Å] with the Rh atom lying on a crystallographic two-fold axis. The folded tetrathia macrocycle is co-ordinated to the Rh^{III} *via* all four S-donors with the angles around the metal being close to octahedral. The conformation of L^2 in *cis*-$[RhCl_2L^2]^+$ is very similar to that observed in the related d^6 complexes *cis*-$[RuCl_2L^2]$,[13] *cis*-$[IrCl_2L^2]^+$.[14] The pattern of Rh–S bond lengths follows that observed for *cis*-$[RuCl_2L^2]$[13] and *cis*-$[IrCl_2L^2]^+$[14] with Rh–S(1) *trans* to Cl(1) being 0.040(2) Å shorter than Rh–S(4) *trans* to S(11). This is consistent with overall π donation from Cl^- to Rh and through to the π-acceptor thioether donor atom.

On the basis of analytical data, and n.m.r., electronic, and mass spectroscopy, the rhodium(III) complex of L^1 is assigned as *cis*-$[RhCl_2L^1]^+$.

Our studies on the complexation of Rh^{III} by the 12-and 14-membered ring macrocycles indicate that the formation of octahedral *cis*-dichloro species is preferred. We have thus far been unable to detect the formation of *trans*-dichloro products, although such species have been isolated for rhodium(III) complexes of the tetra-aza ligands cyclam[9] and tmc (tmc = tetramethylcyclam).[15] This may reflect the smaller hole size of L^2 compared with tetra-aza ligands of the same ring size due to the greater van der Waals radius of S compared with N. These results suggested that tetrathia macrocycles with larger ring sizes might be required to achieve equatorial complexation of the platinum-group metal ions. We therefore undertook a spectroscopic and crystallographic study of $[RhCl_2L^3]PF_6$.

The u.v.-visible spectrum of $[RhCl_2L^3]^+$ shows a *d–d* transition at $\lambda_{max.} = 369$ nm with $\varepsilon_{max.} = 151$ dm^3 mol^{-1} cm^{-1}. The low absorption coefficient for this absorption band is consistent with a *trans* configuration of the Cl^- ligands at Rh^{III}.[9] In addition, the i.r. spectrum of the complex shows peaks at 365 and 305 cm^{-1} tentatively assigned to Rh–S and Rh–Cl stretching vibrations, ν(Rh–S) and ν(Rh–Cl), respectively. The structure of *trans*-$[RhCl_2L^3]^+$ was confirmed by a single-crystal *X*-ray structural determination. Figures 3 and 4 show views of the complex cation which has the Rh atom lying on a crystallographic inversion centre. The tetrathia ligand is bound equatorially to the Rh^{III} [Rh–S(1) 2.348 3(25) and Rh–S(5) 2.348 3(27) Å] with the six-membered chelate rings adopting alternate chair and twist-boat conformations. The Cl^- ligands are mutually *trans* to one another with Rh–Cl(1) 2.339 1(22) Å. The ^{13}C n.m.r. spectrum of the complex in CD_3NO_2 shows four resonances at δ 34.42, 32.27, 23.26, and 21.85 p.p.m. confirming retention of this stereochemistry in solution.

Reaction of $RhCl_3$ with L^4 (L^4 = 1,7,10,13,16-hexathiacyclooctadecane) in refluxing MeCN for 24 h followed by addition of an excess of NH_4PF_6 affords a product tentatively assigned as $[RhCl_2L^4]PF_6$. The fast-atom-bombardment mass spectrum of the isolated product shows peaks at *m/z* 534, 498, and 463 assigned to $[^{103}Rh^{35}Cl_2L^4 + H]^+$, $[^{103}Rh^{35}ClL^4]^+$, and $[^{103}RhL^4]^+$ respectively. Molecular peaks corresponding to dimeric species have not been observed. Identification of this product has been difficult since the analytical data were intermediate between the formulations $[RhCl_2L^4]PF_6$ and $[RhClL^4][PF_6]_2$. Weak bands are observed in the i.r. spectrum at 320 and 355 cm^{-1} assigned to Rh–S or Rh–Cl stretching vibrations. However, from our limited experimental data on this system it appears that the formation of the homoleptic cation $[RhL^4]^{3+}$ is inhibited. This may be due to conformational constraints of the sexidentate macrocycle binding to a kinetically inert second-row (3+) transition-metal ion. In addition, deprotonation and ring opening of co-ordinated L^4 can occur in the presence of Rh^{III}, thus reducing the potential yield of $[RhL^4]^+$.

Cyclic voltammetry of *cis*-$[RhCl_2L]^+$ (L = L^1 or L^2) in MeCN (0.1 mol dm^{-3} $NBu^n{}_4PF_6$) at platinum electrodes shows an irreversible reduction for each complex at $E_{pc} = -1.10$ and -1.18 V respectively, while for *trans*-$[RhCl_2L^3]^+$ a quasi-reversible reduction is observed at $E_{\frac{1}{2}} = -0.83$ V ($E_{pc} = -1.08$ V) *vs.* ferrocene–ferrocenium. No oxidation was observed for these complexes in the range 0—2.0 V *vs.* ferrocene–ferrocenium. Coulometry at 298 K indicated that the reduction of *cis*-$[RhCl_2L^2]^+$ and *trans*-$[RhCl_2L^3]^+$ is, in each case, a one-electron process affording a highly reactive radical species. The e.s.r. spectrum of the reduction product of *trans*-$[RhCl_2L^2]^+$, measured as a MeCN glass at 77 K, shows a weak signal with $g_1 = 2.230$, $g_2 = 2.090$, and $g_3 = 2.003$ tentatively assigned to the formation, in low yield, of a d^7 rhodium(II) species. These reduction products are, however, extremely reactive, and their further characterisation was inhibited by decomposition reactions in solution. Coulometry showed the reduction of *cis*-$[RhCl_2L^1]^+$ to involve up to two electrons, with rapid decomposition of the redox product occurring in solution. The formation of reactive rhodium(II) species *via* loss of Cl^- ions from the metal centre is likely to be involved in these redox reactions. Indeed, a $Cl^{-/0}$ couple is observed in the cyclic voltammogram of the reaction solution following reduction of $[RhCl_2L^2]^+$. Interestingly, the complex cation *trans*-$[RhCl_2(tmc)]^+$ shows a quasi-reversible Rh^{III}–Rh^{II} couple at -0.99 V *vs.* ferrocene–ferrocenium under the same conditions.[15] This again may reflect the greater cavity size of the N_4 ligand *versus* its S_4 analogue, coupled with destabilisation of Rh^I in a tetra-aza co-ordination sphere. The synthesis of $[RhL^2]^+$ has been reported previously;[16] the single-crystal *X*-ray structure of this species shows the Rh atom lying 0.133(2) Å above the S_4 plane of the macrocycle with additional intermolecular Rh···Rh and Rh···S interactions being observed in the solid state.[16] Current work is aimed at elucidating the mechanisms of reduction of $[RhCl_2L]^+$ (L = tmc, L^1, L^2, or L^3) and to probe the intermediacy of monomeric and dimeric rhodium(II) species in these reactions.

Experimental

Infrared spectra were measured as Nujol mulls, KBr and CsI discs using a Perkin-Elmer 598 spectrometer over the range 200—4 000 cm^{-1}. U.v.-visible spectra were measured in quartz cells using Perkin-Elmer Lambda 9 and Philips Scientific SP8-400 spectrophotometers. Microanalyses were performed by the Edinburgh University Chemistry Department microanalytical service. Electrochemical measurements were performed on a Bruker E310 Universal Modular Polarograph. All readings were taken using a three-electrode potentiostatic system in acetonitrile containing 0.1 mol dm^{-3} $NBu^n{}_4PF_6$ or $NBu^n{}_4BF_4$ as supporting electrolyte. Cyclic voltammetric measurements were carried out using a double platinum electrode and a Ag–AgCl reference electrode. All potentials are quoted *versus* ferrocene–ferrocenium. Mass spectra were run by electron impact on a Kratos MS 902 and by fast-atom-bombardment (f.a.b.) on a Kratos MS 50TC spectrometer. Proton and ^{13}C n.m.r. spectra were obtained on Bruker WP80 and WP200 instruments.

Synthesis of cis-$[RhCl_2L^1]PF_6$.—Reaction of $RhCl_3\cdot3H_2O$ (0.043 g, 1.66×10^{-4} mol) in water (5 cm^3) with L^1 (0.04 g, 1.66×10^{-4} mol) in refluxing MeOH (130 cm^3) for 2 h afforded a bright yellow solution. Addition of an excess of NH_4PF_6 gave the product as a yellow precipitate which was collected and recrystallised from MeCN and dried *in vacuo*. Yield = 0.075 g, 81% {Found: C, 17.2; H, 2.90; S, 23.1. Calc. for $[RhCl_2L^1]PF_6$: C, 17.2; H, 2.90; S, 22.9%}. U.v.-visible spectrum (MeCN): $\lambda_{max.}$ 401 ($\varepsilon_{max.}$ = 1 781), 300 (sh) (1 165), and 250 nm (21 920 dm^3 mol^{-1} cm^{-1}). F.a.b. mass spectrum (matrix, 3-nitrobenzyl alcohol): Found *m/z* 413, 378; calc. for $[^{103}Rh^{35}Cl_2L^1]^+$ *m/z* 413, for $[^{103}Rh^{35}ClL^1]^+$ 378. N.m.r. (CD_3CN, 298 K): ^1H (80 MHz), δ 3.3—4.2 (16 H, CH_2, m); ^{13}C (50.32 MHz), δ 44.41, 41.03, 36.08, and 35.16 p.p.m. (CH_2). Infrared spectrum (KBr disc): 2 990m, 2 925m, 1 410vs, 1 280m, 1 265m, 1 150w, 1 120w, 1 090m, 990w, 950w, 925m, 840vs, 555vs, 360m, 345m, 330m, 290m, and 270w cm^{-1}.

Synthesis of cis-$[RhCl_2L^2]PF_6$.—To a refluxing solution of L^2 (0.061 g, 2.28×10^{-4} mol) in MeOH (100 cm^3) was added $RhCl_3\cdot3H_2O$ (0.06 g, 2.28×10^{-4} mol) in water (5 cm^3). The reaction mixture was refluxed for 1 h under N_2 to afford a bright yellow solution which was filtered to remove insoluble chloro-bridged polymer. Addition of an excess of NH_4PF_6 in MeOH yielded a yellow precipitate, which was collected, washed with methanol, recrystallised from MeCN, and dried *in vacuo*. Yield = 0.1 g, 75%. As reported by Busch and co-workers,[2] it is important that addition of $RhCl_3$ should occur to a refluxing solution of the ligand to minimise the formation of chloro-bridged polymer species. Elemental analysis {Found: C, 20.4; H, 3.4; S, 21.4. Calc. for $[RhCl_2L^2]PF_6$: C, 20.4; H, 3.4; S, 21.8%}. U.v.-visible spectrum (MeCN): $\lambda_{max.}$ = 362 ($\varepsilon_{max.}$ = 949), 319 (765), and 260nm (10 370 dm^3 mol^{-1} cm^{-1}). Infrared spectrum (KBr disc): 3 000m, 2 940w, 2 920w, 1 430vs, 1 420vs, 1 400m, 1 360w, 1 300w, 1 280w, 1 270m, 1 240w, 1 190w, 1 160w, 1 130m, 1 100w, 1 020w, 1 010w, 985m, 930m, 840vs, 555vs, 460w, 370w, 310m, and 280m cm^{-1}.

Synthesis of cis-$[RhCl_2L^2]BPh_4$.—The BPh_4^- salt was

Table 1. Bond lengths (Å), angles and torsion angles (°) with standard deviations for *cis*-$[RhCl_2L^2]^+$

Rh–Cl(1)	2.3836(12)	C(2)–C(3)	1.509(8)
Rh–S(1)	2.2870(12)	C(3)–S(4)	1.827(5)
Rh–S(4)	2.3275(12)	S(4)–C(5)	1.816(6)
S(1)–C(2)	1.814(5)	C(5)–C(6)	1.525(8)
S(1)–C(14)	1.806(5)	C(6)–C(7)	1.510(8)
Cl(1)–Rh–S(1)	92.00(4)	Rh–S(1)–C(14)	108.96(18)
Cl(1)–Rh–S(4)	86.51(4)	C(2)–S(1)–C(14)	105.32(25)
Cl(1)–Rh–Cl(2)	92.01(4)	S(1)–C(2)–C(3)	107.7(4)
Cl(1)–Rh–S(8)	174.25(4)	C(2)–C(3)–S(4)	109.3(4)
Cl(1)–Rh–S(11)	88.72(4)	Rh–S(4)–C(3)	103.19(17)
S(1)–Rh–S(4)	87.40(4)	Rh–S(4)–C(5)	111.43(19)
S(1)–Rh–S(8)	84.32(4)	C(3)–S(4)–C(5)	103.1(3)
S(1)–Rh–S(11)	97.71(4)	S(4)–C(5)–C(6)	118.2(4)
S(4)–Rh–S(8)	97.71(4)	C(5)–C(6)–C(7)	115.9(5)
S(4)–Rh–S(11)	173.13(4)	C(6)–C(7)–S(8)	108.7(4)
Rh(1)–S(1)–C(2)	100.37(18)		
Cl(1)–Rh–S(1)–C(2)	60.09(18)	Cl(2)–Rh–S(4)–C(3)	175.39(18)
Cl(1)–Rh–S(1)–C(14)	−50.21(19)	Cl(2)–Rh–S(4)–C(5)	65.42(20)
S(4)–Rh–S(1)–C(2)	−26.32(18)	S(8)–Rh–S(4)–C(3)	83.55(18)
S(4)–Rh–S(1)–C(14)	−136.63(19)	S(8)–Rh–S(4)–C(5)	−26.42(21)
Cl(2)–Rh–S(1)–C(2)	−74.0(5)	S(11)–Rh–S(4)–C(3)	−138.6(4)
Cl(1)–Rh–S(8)–C(7)	175.7(4)	S(11)–Rh–S(4)–C(5)	111.4(4)
S(8)–Rh–S(1)–C(2)	−124.35(18)	C(2)–S(1)–C(14)–C(13)	−173.9(4)
S(8)–Rh–S(1)–C(14)	125.36(19)	S(1)–C(2)–C(3)–S(4)	−60.9(4)
S(11)–Rh–S(1)–C(2)	149.07(18)	C(2)–C(3)–S(4)–Rh	34.5(4)
S(11)–Rh–S(1)–C(14)	38.77(19)	C(2)–C(3)–S(4)–C(5)	150.6(4)
Cl(1)–Rh–S(4)–C(3)	−92.52(18)	Rh–S(4)–C(5)–C(6)	40.0(5)
Cl(1)–Rh–S(4)–C(5)	157.51(20)	C(3)–S(4)–C(5)–C(6)	−70.1(5)
S(1)–Rh–S(4)–C(3)	−0.36(18)	S(4)–C(5)–C(6)–C(7)	−70.9(6)
S(1)–Rh–S(4)–C(5)	−110.33(20)	C(5)–C(6)–C(7)–S(8)	85.1(5)

Table 2. Fractional co-ordinates with standard deviations for *cis*-$[RhCl_2L^2]^+$

Atom	*x*	*y*	*z*
Rh	0.0	0.453 14(4)	0.25
Cl(1)	0.078 34(11)	0.599 69(10)	0.346 99(7)
S(1)	0.056 36(11)	0.303 09(10)	0.341 15(7)
C(2)	−0.034 3(5)	0.341 5(5)	0.432 5(3)
C(3)	−0.168 9(5)	0.349 8(5)	0.402 5(3)
S(4)	−0.185 58(12)	0.465 48(9)	0.321 58(8)
C(5)	−0.316 7(5)	0.414 5(5)	0.255 4(4)
C(6)	−0.298 5(5)	0.306 0(5)	0.199 4(3)
C(7)	−0.216 9(5)	0.323 3(5)	0.124 1(3)
P(1)	0.0	0.0	0.5
F(1)	0.112 7(3)	0.070 7(3)	0.461 85(24)
F(2)	0.094 4(4)	−0.063 1(3)	0.564 91(25)
F(3)	−0.018 8(4)	0.103 9(3)	0.565 01(21)

prepared by using $NaBPh_4$ instead of $NaPF_6$ in the above preparation {Found: C, 53.4; H, 5.4; Cl, 9.7; S, 16.9. Calc. for $[RhCl_2L^2]BPh_4$: C, 53.6; H, 5.25; Cl, 9.3; S, 16.8%}. F.a.b. mass spectrum (3-NOBA matrix): found: *m/z* 441, 406, and 370; calc. for $[^{103}Rh^{35}Cl_2L^2]^+$ *m/z* 441, for $[^{103}Rh^{35}ClL^2]^+$ 406, and for $[^{103}RhL^2 - H]^+$ 370. N.m.r. (CD_3CN): ^1H (80 MHz, 298 K), δ 6.8—7.7 (20 H, BPh_4^-, m) and 2.5—3.6 (20 H, CH_2, m); ^{13}C (50.32 MHz, 333 K), δ 38.31, 30.10, 29.95, 29.85, and 23.84 p.p.m. (CH_2).

X-Ray Structure Determination of cis-$[RhCl_2L^2]PF_6$.—A bright yellow crystal (0.50 × 0.50 × 0.30 mm) suitable for *X*-ray analysis was obtained by recrystallisation from MeCN.

Crystal data. $C_{10}H_{20}Cl_2RhS_4{}^+PF_6{}^-$, $M = 587.284$, monoclinic, space group $C2/c$, $a = 10.746(8)$, $b = 11.298(5)$, $c = 15.708(8)$ Å, $\beta = 92.00(5)°$, $U = 1\,905.92$ Å^3 [from diffractometer angles for 12 centred reflections with $2\theta = 30—33°$ ($\bar{\lambda} = 0.710\,73$ Å)], $D_c = 2.047$ g cm^{-3}, $Z = 4$, $F(000) = 1\,168$, $\bar{\lambda}(\text{Mo-}K_\alpha) = 0.710\,73$ Å, $\mu = 16.5$ cm^{-1}.

Data collection and processing. Stoë STADI-4 four-circle diffractometer. After determination of an accurate orientation matrix, 1 320 independent data (h −12 to 12, k 0 to 12, l 0 to 17) were collected to $2\theta = 45°$ using ω—θ scans with ω scan width (2.0 + 0.35tanθ)°. Data reduction yielded 1 161 reflections with $F \geqslant 6\sigma(F)$ which were used for solution and refinement of the structure. No significant crystal decay, no absorption correction.

Structure analysis and refinement. The position of the Rh atom was obtained from a Patterson synthesis. Subsequent iterative rounds of least-squares refinement and difference Fourier synthesis[17] located all remaining atoms, including H atoms which were then refined positionally but with a fixed, isotropic thermal parameter ($U = 0.08$ Å^2). All non-H atoms were refined anisotropically. Both the PF_6^- counter ion and the $[RhCl_2L^2]^+$ cation were ordered. The weighting scheme $w^{-1} = \sigma^2(F) + 0.000\,076F^2$ gave satisfactory analyses. At convergence, $R, R' = 0.0311$ and 0.0461 respectively for 141 parameters, $S = 1.191$. The maximum and minimum residues in the final ΔF synthesis were +0.84 and −0.50 e Å^{-3} respectively. The Rh atom lies on a crystallographic two-fold axis while the P of the PF_6^- counter ion occupies a crystallographic inversion centre. Illustrations were prepared using ORTEP,[18] molecular geometry calculations utilised CALC,[19] and scattering factor data were taken from ref. 20. Bond lengths, angles, torsion angles, and fractional co-ordinates are given in Tables 1 and 2.

Additional material available from the Cambridge Crystallographic Data Centre comprises H-atom co-ordinates and thermal parameters.

Synthesis of trans-$[RhCl_2L^3]PF_6$.—Reaction of $RhCl_3\cdot3H_2O$ (0.035 g, 1.35 × 10^{-4} mol) in water (5 cm^3) with L^3 (0.04 g, 1.35 × 10^{-4} mol) in refluxing EtOH (150 cm^3) for 1 h afforded a

Table 3. Bond lengths (Å), angles and torsion angles (°) with standard deviations for *trans*-$[RhCl_2L^3]^+$

Rh–Cl(1)	2.339 1(22)	S(5)–C(6)	1.800(14)
Rh–S(1)	2.348 3(25)	C(2)–C(3)	1.517(21)
Rh–S(5)	2.348 3(27)	C(3)–C(4)	1.514(22)
S(1)–C(2)	1.811(13)	C(6)–C(7)	1.507(22)
S(1)–C(8′)	1.832(14)	C(7)–C(8)	1.501(22)
S(5)–C(4)	1.807(15)		
Cl(1)–Rh–S(1)	92.88(8)	C(4)–S(5)–C(6)	97.2(6)
Cl(1)–Rh–S(5)	92.72(8)	S(1)–C(2)–C(3)	112.1(10)
S(1)–Rh–S(5)	90.31(9)	C(2)–C(3)–C(4)	114.8(13)
Rh–S(1)–C(2)	110.1(4)	S(5)–C(4)–C(3)	115.1(11)
Rh–S(1)–C(8′)	104.5(5)	S(5)–C(6)–C(7)	111.8(10)
C(2)–S(1)–C(8′)	97.1(6)	C(6)–C(7)–C(8)	115.0(13)
Rh–S(5)–C(4)	110.0(5)	S(1′)–C(8)–C(7)	112.4(10)
Rh–S(5)–C(6)	105.1(4)		
Cl(1)–Rh–S(1)–C(2)	45.3(4)	Rh–S(1)–C(2)–C(3)	65.6(10)
Cl(1)–Rh–S(1)–C(8′)	−58.0(5)	C(8′)–S(1)–C(2)–C(3)	173.9(11)
S(5)–Rh–S(1)–C(2)	−47.5(4)	Rh–S(1′)–C(8)–C(7)	80.5(11)
S(5)–Rh–S(1)–C(8′)	−150.8(5)	C(2′)–S(1′)–C(8)–C(7)	−166.6(11)
Cl(1)–Rh–S(1′)–C(8)	−122.0(5)	Rh–S(5)–C(4)–C(3)	−61.7(12)
S(5)–Rh–S(1′)–C(8)	−29.2(5)	C(6)–S(5)–C(4)–C(3)	−170.7(11)
Cl(1)–Rh–S(5)–C(4)	−47.9(5)	Rh–S(5)–C(6)–C(7)	81.4(10)
Cl(1)–Rh–S(5)–C(6)	55.8(5)	C(4)–S(5)–C(6)–C(7)	−165.5(11)
S(1)–Rh–S(5)–C(4)	45.0(5)	S(1)–C(2)–C(3)–C(4)	−76.1(14)
S(1)–Rh–S(5)–C(6)	148.7(5)	C(2)–C(3)–C(4)–S(5)	74.9(15)
S(1′)–Rh–S(5)–C(4)	−135.0(5)	S(5)–C(6)–C(7)–C(8)	−42.8(16)
S(1′)–Rh–S(5)–C(6)	−31.3(5)	C(6)–C(7)–C(8)–S(1′)	−44.0(16)

Primed atoms are related to their unprimed equivalents by inversion through $(\frac{1}{2}, \frac{1}{2}, \frac{1}{2})$.

Table 4. Atomic co-ordinates with standard deviations for *trans*-$[RhCl_2L^3]^+PF_6^-$

Atom	*x*	*y*	*z*
Rh	0.5000	0.5000	0.5000
Cl(1)	0.626 75(18)	0.559 42(22)	0.405 95(12)
S(1)	0.501 37(20)	0.690 42(22)	0.563 09(16)
S(5)	0.343 48(19)	0.556 0(3)	0.410 11(14)
C(2)	0.489 2(12)	0.807 3(9)	0.484 9(8)
C(3)	0.376 5(15)	0.804 2(13)	0.433 8(11)
C(4)	0.363 9(11)	0.705 1(15)	0.369 5(8)
C(6)	0.358 1(10)	0.474 4(16)	0.315 7(6)
C(7)	0.316 8(11)	0.346 6(20)	0.320 7(10)
C(8)	0.350 9(10)	0.283 4(12)	0.400 9(10)
P(1)	0.5000	0.021 2(3)	0.2500
F(1)	0.611 8(5)	0.022 0(6)	0.205 2(4)
F(2)	0.434 0(7)	0.025 7(11)	0.164 0(5)
F(3)	0.5000	−0.114 4(10)	0.2500
F(4)	0.5000	0.160 9(10)	0.2500

bright yellow solution. Addition of an excess of NH_4PF_6 gave the product as a yellow precipitate which was collected and recrystallised from MeCN and dried *in vacuo*. Yield = 0.060 g, 72% {Found: C, 23.6; H, 3.90. Calc. for $[RhCl_2L^3]PF_6$: C, 23.4; H, 3.95%}. U.v.–visible spectrum (MeCN): $\lambda_{max.}$ = 369 ($\varepsilon_{max.}$ = 151), 278 (38 290), and 232 nm (18 930 dm^3 mol^{-1} cm^{-1}). F.a.b. mass spectrum (3-NOBA matrix): found *m/z* 469, 434, and 399; calc. for $[^{103}Rh^{35}Cl_2L^3]^+$ *m/z* 469, for $[^{103}Rh^{35}ClL^3]^+$ 434, and for $[^{103}RhL^3]^+$ 399. N.m.r. (298 K): ^1H (CD_3CN, 80 MHz), δ 2.3—3.7 (24 H, CH_2, m); ^{13}C (CD_3NO_2, 50.32 MHz), δ 34.42, 32.27, 23.26, and 21.85 p.p.m. (CH_2). Infrared spectrum (KBr disc): 2 980w, 2 920m, 2 840w, 1 430vs, 1 405m, 1 310m, 1 290m, 1 255w, 1 240m, 1 195w, 1 160m, 1 120w, 1 080w, 1 020m, 840vs, 555vs, 365m, 305m, and 270w cm^{-1}.

X-Ray Structure Determination of trans-$[RhCl_2L^3]PF_6$.—A bright yellow crystal (0.23 × 0.15 × 0.15 mm) suitable for *X*-ray analysis was obtained by recrystallisation from MeCN.

Crystal data. $C_{12}H_{24}Cl_2RhS_4{}^+PF_6{}^-$, M = 615.34, monoclinic, space group $C2/c$, a = 11.950 7(20), b = 11.105 5(15), c = 16.206 7(18) Å, β = 95.197(21)°, U = 214 2.08 Å^3 [from 2θ values of 30 reflections measured at ±ω (2θ = 21—30°, $\bar{\lambda}$ = 0.710 73 Å)], D_c = 1.908 g cm^{-3}, Z = 4, $F(000)$ = 1 232, $\bar{\lambda}$(Mo-K_α) = 0.710 73 Å, μ = 14.72 cm^{-1}.

Data collection and processing. Stoë STADI-4 four-circle diffractometer. After determination of an accurate orientation matrix, 1 549 independent data (h −12 to 12, k 0 to 11, l 0 to 17) were collected to 2θ = 45° using ω—2θ scans with ω scan width (1.20 + 0.347tanθ)°. Data reduction yielded 1 067 reflections with $F \geqslant 6\sigma(F)$ which were used for solution and refinement of the structure. No significant crystal decay, no absorption correction.

Structure analysis and refinement. Analysis of intensity statistics clearly indicated the position of the Rh atom; using this information as input DIRDIF[21] successfully located the Cl, S, and P atoms. Subsequent interative rounds of least-squares refinement and difference Fourier synthesis[17] located all other non-H atoms. All non-H atoms were refined anisotropically; H atoms were included in fixed, calculated positions.[17] The weighting scheme $w^{-1} = \sigma^2(F) + 0.000\,475F^2$ gave satisfactory analyses. At convergence, R,R' = 0.0396 and 0.0536 respectively for 121 parameters, S = 1.202. The maximum and minimum residues in the final ΔF synthesis were +0.80 and − 0.51 e Å^{-3} respectively. The Rh atom sits on an inversion centre, with the $PF_6{}^-$ counter ion having a two-fold axis through the P and two F atoms. Illustrations were prepared using ORTEP,[18] molecular geometry calculations utilised CALC,[19] and scattering factor data were taken from ref. 20. Bond lengths, angles, torsion angles, and fractional co-ordinates are given in Tables 3 and 4.

Acknowledgements

We thank the S.E.R.C. for support, and Johnson Matthey plc for generous loans of platinum metals.

References

1 M. Schröder, *Pure Appl. Chem.*, 1988, **60**, 517; M. N. Bell, A. J. Blake, R. O. Gould, A. J. Holder, T. I. Hyde, A. J. Lavery, G. Reid, and M. Schröder, *J. Inclusion Phenomena*, 1987, **5**, 169 and refs. therein.

2 K. Travis and D. H. Busch, *Inorg. Chem.*, 1974, **13**, 2591; W. D. Lemke, K. E. Travis, N. E. Takvoryan, and D. H. Busch, *Adv. Chem. Ser.*, 1977, **150**, 358.

3 R. E. DeSimone and M. D. Glick, *J. Am. Chem. Soc.*, 1976, **98**, 762.

4 R. E. DeSimone and M. D. Glick, *J. Am. Chem. Soc.*, 1975, **97**, 942.

5 N. W. Alcock, N. Herron, and P. Moore, *J. Chem. Soc., Chem. Commun.*, 1976, 886.

6 P. H. Davis, K. L. White, and R. L. Bedford, *Inorg. Chem.*, 1975, **14**, 1753.

7 M. D. Glick, D. P. Gavel, L. L. Diaddario, and D. B. Rorabacher, *Inorg. Chem.*, 1976, **15**, 1190.

8 E. R. Dockal, L. L. Diaddario, M. D. Glick, and D. B. Rorabacher, *J. Am. Chem. Soc.*, 1977, **99**, 4530.

9 E. J. Bounsall and S. R. Koprich, *Can. J. Chem.*, 1970, **44**, 1481; P. K. Bhattacharya, *J. Chem. Soc., Dalton Trans.*, 1980, 810; M. E. Sosa and M. L. Tobe, *ibid.*, 1986, 427; M. J. Rosales, M. E. Sosa, and M. L. Tobe, *J. Coord. Chem.*, 1987, **16**, 59.

10 A. J. Blake, T. I. Hyde, R. S. E. Smith, and M. Schröder, *J. Chem. Soc., Chem. Commun.*, 1986, 334.

11 A. J. Blake, T. I. Hyde, and M. Schröder. *J. Chem. Soc., Dalton Trans.*, 1988, 1165.

12 T. Yoshida, T. Adachi, T. Ueda, M. Watanabe, M. Kaminaka, and T. Higuchi, *Angew. Chem.*, 1987, **99**, 1182; *Angew. Chem., Int. Ed. Engl.*, 1987, **26**, 1171.

13 T. F. Lai and C. K. Poon, *J. Chem. Soc., Dalton Trans.*, 1982, 1465.

14 A. J. Blake, R. O. Gould, G. Reid, and M. Schröder, *J. Organomet. Chem.*, 1988, **356**, 389.

15 A. J. Blake, G. Reid, and M. Schröder, *J. Chem. Soc., Dalton Trans.*, 1988, 1561.

16 T. Yoshida, T. Ueda, T. Adachi, K. Yamamoto, and T. Higuchi, *J. Chem. Soc., Chem. Commun.*, 1985, 1137.

17 SHELX 76, Program for Crystal Structure Determination, G. M. Sheldrick, University of Cambridge, 1976.

18 ORTEP II, interactive version, P. D. Mallinson and K. W. Muir, *J. Appl. Cryst.*, 1985, **18**, 51.

19 CALC, Fortran 77 version, R. O. Gould and P. Taylor, University of Edinburgh, 1985.

20 D. T. Cromer and J. L. Mann, *Acta Crystallogr., Sect. A*, 1968, **24**, 321.

21 DIRDIF, P. T. Beurskens, W. P. Bosman, H. M. Doesbury, Th. E. M. van den Hark, P. A. J. Prick, J. H. Noordik, G. Beurskens, R. O. Gould, and V. Parthasarathia, 'Applications of Direct Methods to Difference Structure Factors,' University of Nijmegen, 1983.

Received 8*th July* 1988; *Paper* 8/02739K